ELSEVIER

Contents lists available at ScienceDirect

# **Advanced Engineering Informatics**

journal homepage: www.elsevier.com/locate/aei



# Full length article

# Artificial intelligence-enhanced seismic response prediction of reinforced concrete frames



Huan Luo <sup>a,b,\*</sup>, Stephanie German Paal <sup>c</sup>

- <sup>a</sup> Hubei Key Laboratory of Disaster Prevention and Mitigation, Yichang, HuBei 443002, China
- <sup>b</sup> College of Civil Engineering & Architecture, China Three Gorges University, Yichang, HuBei 443002, China
- <sup>c</sup> Zachry Department of Civil & Environmental Engineering, Texas A&M University, College Station, TX 77843, USA

# ARTICLE INFO

# Keywords: Artificial intelligence-enhanced shear building model Machine learning Data-driven modeling Fiber model Reinforced concrete frames Nonlinear seismic response prediction

# ABSTRACT

Existing physics-based modeling approaches do not have a good compromise between performance and computational efficiency in predicting the seismic response of reinforced concrete (RC) frames, where high-fidelity models (e.g., fiber-based modeling method) have reasonable predictive performance but are computationally demanding, while more simplified models (e.g., shear building model) are the opposite. This paper proposes a novel artificial intelligence (AI)-enhanced computational method for seismic response prediction of RC frames which can remedy these problems. The proposed AI-enhanced method incorporates an AI technique with a shear building model, where the AI technique can directly utilize the real-world experimental data of RC columns to determine the lateral stiffness of each column in the target RC frame while the structural stiffness matrix is efficiently formulated via the shear building model. Therefore, this scheme can enhance prediction accuracy due to the use of real-world data while maintaining high computational efficiency due to the incorporation of the shear building model. Two data-driven seismic response solvers are developed to implement the proposed approach based on a database including 272 RC column specimens. Numerical results demonstrate that compared to the experimental data, the proposed method outperforms the fiber-based modeling approach in both prediction capability and computational efficiency and is a promising tool for accurate and efficient seismic response prediction of structural systems.

#### 1. Introduction

As a common structural system, reinforced concrete (RC) frame buildings (composed of various RC structural components including beams and columns) are widely distributed throughout the world. In high seismic regions, RC frames undergoing seismic loads may behave nonlinearly. It is necessary to accurately predict the nonlinear response of RC frames under future earthquakes, as the seismic demand and capacity of the RC frames can be quantified from the predicted nonlinear seismic response [15,29]. The predicted seismic demand and capacity of the RC frames can help people take necessary precautions (e.g., strengthening and retrofitting) to reduce their collapse risk prior to an earthquake [32]. One of the most common ways to predict the nonlinear seismic response of an RC frame is to perform nonlinear time-history analyses using existing physics-based approaches (e.g., finite element method) [5,7,33]. The prediction accuracy of the nonlinear seismic response of RC frame buildings is closely related to the structural

stiffness, as the structural stiffness directly relates the external forces to the deformations of the building [44]. Structural stiffness is a matrix form in the case of structural systems that have multi-degrees of freedom (MDOF) for dynamic analysis. However, existing physics-based modeling approaches do not generally have a good compromise between predictive performance and computational efficiency. High-fidelity models (e.g., fiber-based modeling approaches) utilize the constitutive models at the material level to compute the structural stiffness matrix and thus have reasonable predictive performance but are computationally demanding. Conversely, more simplified models (e.g., shear building model) may be computationally efficient, but employ simple empirical constitutive relations at the structural member level to calculate the stiffness matrix and therefore do not have performance as good as high-fidelity models [44].

Typically, the formulation of the structural stiffness matrix for high-fidelity models (e.g., fiber-based modeling approaches) involves integrations from section stiffness to element stiffness and finally through

<sup>\*</sup> Corresponding author at: College of Civil Engineering & Architecture, China Three Gorges University, Yichang, HuBei 443002, China. E-mail address: hluo@ctgu.edu.cn (H. Luo).

to structure stiffness based on material constitutive models. But, for simplified models (e.g., shear building model), the formulation of the structural stiffness matrix can be direct assembled from member to member based on empirical constitutive models at the member level. Furthermore, when involving nonlinear analysis, both high-fidelity and simplified models need to update the stiffness matrix at each load step, leading to much higher computational cost for high-fidelity models than simplified models. However, compared to high-fidelity models, empirical constitutive models utilized by simplified approaches at the member level may not be able to fully capture the experimentally observed behavior. This means that the analytical results predicted by simplified models have much more evident discrepancies with the experimentally observed behavior than those predicted by high-fidelity models. Therefore, a novel computational methodology for efficient and accurate seismic response prediction of RC frames is needed.

Recently, with more and more data available, data science has become a newly burgeoning field and has been successfully applied in many engineering and science disciplines including civil engineering [1,37] [49]. In data science, physical behavior can be derived directly from real-world big data, the rigorous physical theoretical inference is no longer required, and relations inferred from empirical models will be less informative than those directly reflected in the data [34]. In data science approaches, knowledge is extracted from the data (also called the training dataset) by using advanced artificial intelligence (AI) techniques or statistical learning approaches (e.g., non-parametric machine learning methods) without any human assumptions or inference. This knowledge is typically expressed in a specific mathematic form which is then employed to directly relate the input predictors to the output responses with high generalization performance and computational efficiency. These types of approaches have been employed more often in recent years in structural earthquake engineering applications to achieve good predictive performance and high computational efficiency [6,21,22,28,27,36,47,49,10,11][17]. However, these studies only focus on predicting the strength and deformation capacity of various structural components.

Additionally, although many studies have successfully adopted AI techniques (e.g., neural network-based methods) to accurately and efficiently predict the seismic performance of structural systems, they use the ground motions and corresponding seismic response data (simulated or measured) to develop the corresponding nonlinear relations [19], [48,53]. On one hand, simulated data is less meaningful and informative than experimentally measured data, and measured data is very limited. On the other hand, seismic response data does not relate the structural features to the structural response, leading to limited predictive capability for new structures with changes in structural features. To solve these problems, we propose a novel AI-enhanced method, which links structural features to experimental data by formulating the stiffness matrix directly from real-world experimental data of structural components in the RC frames, to predict the nonlinear seismic response of RC frames. The proposed method is more accurate and efficient than existing widely-used traditional fiber-based modeling approaches.

The rest of this paper is organized as follows. Section 2 serves as the literature review to discuss existing AI-based methods in predicting structural seismic response for illustrating the computational novelty of the proposed method. Section 3 presents the methodology of a novel AI-enhanced method for seismic response prediction of RC frames. Section 4 describes the column dataset used in the proposed method. Section 5 presents a comparison and discussion of the numerical results for RC frames under both quasi-static cyclic loading and dynamic earthquake ground motions. The conclusions are made in Section 6.

# 2. Literature review

In the structural and earthquake engineering domain, many researchers have focused on using artificial intelligence (AI) techniques (e. g., machine learning (ML)) to identify structural damage and predict the

strength and deformation capacity of various structural components, such as RC beams, slabs, columns, walls, and beam-column joints. For example, computer vision-based methods were used to automatically recognize structural damage and evaluate structural performance based on images of post-earthquake structures [18,12,13,35,20,55]; datadriven methods were proposed to evaluate the post-earthquake structural safety state [14,52]; support vector machines for regression (SVMR) [45]) and its extension version, least squares SVMR (LS-SVMR) [43] were used to predict the shear strength of RC deep beams [6,36], the punching shear capacity of fiber-reinforced polymer (FRP) RC slabs [47], the backbone curve and drift capacity of RC columns [21,22], and the dynamic response of structures [56], as well as to reduce the sample bias of small datasets [23] and predict the strength in the context of missing data [24]. In these studies, the training sets are collected from real-world experimental data, and the results predicted from the AIbased methods show much better agreement with experimental data than those obtained by traditional physics-based approaches. However, system-level seismic response prediction using the component-level experimental data based on AI techniques has not yet been fully explored. This is because a given structural system consists of various components (e.g., beams, columns, and walls), and this complex nature makes it difficult to establish a system-level training set. Moreover, system-level physical experimental data is also limited due to the expensive nature of such tests [57,58].

Several researchers have used alternative ways to achieve datadriven prediction for structural systems under earthquakes. Specifically, they use simulated or measured seismic response data to develop a nonlinear functional mapping between ground motions and corresponding seismic response [19]; Perez-Ramirez et al. 2019; [48,53] (Zhang et al., 2020a,b). Zhang et al [53] proposed a deep learning (DL)based approach to predict the nonlinear seismic response of a structural system. In this method, for a target structural system, a training set where the predictors are ground motion-related information (e.g., ground acceleration, velocity, and displacement) and the response variables are the structural response-related information (e.g., story acceleration, velocity, and displacement) is used to train a DL model. The DL model can then be used to predict the structural response for the target system subjected to a new ground motion. The structural response data in the training set is either measured by sensors or simulated by nonlinear time-history analyses for the target system under multiple ground motion records. Similar schemes were also devised by Guarize et al. [16] for seismic response prediction of marine structures, by Lagaros and Papadrakakis [19] for seismic response prediction of buildings, by Wu and Jahanshahi [48] for seismic response prediction of a 3-story steel frame, and by Zhang et al. [54] and Yu et al. [51] for physics-guided seismic response prediction. However, this type of AIbased method is only valid for predicting the same structural system where the training set including ground motion records and corresponding structural response is used but may produce significant errors when predicting for another structure where structural features change significantly. This is because the training set does not relate any structural features (e.g., structural geometry, material properties, or reinforcement details) to the structural response, and the structural seismic behavior varies significantly when certain structural features change. Therefore, once some structural features change, the training set will no longer be valid for the new structure.

From the review of existing AI-based methods for seismic response prediction of structural systems, it can be concluded that the main problem for existing AI-based methods is that they do not relate the structural features to the experimental data, and thus the trained AI models cannot capture the variation in response for a new structure. Different from existing methods, this paper proposes a novel AI-enhanced computational method to solve this problem. The proposed method can relate the structural features to the experimental data for accurate and efficient nonlinear seismic response prediction of RC frames by coupling the AI technique with the mechanical model. The

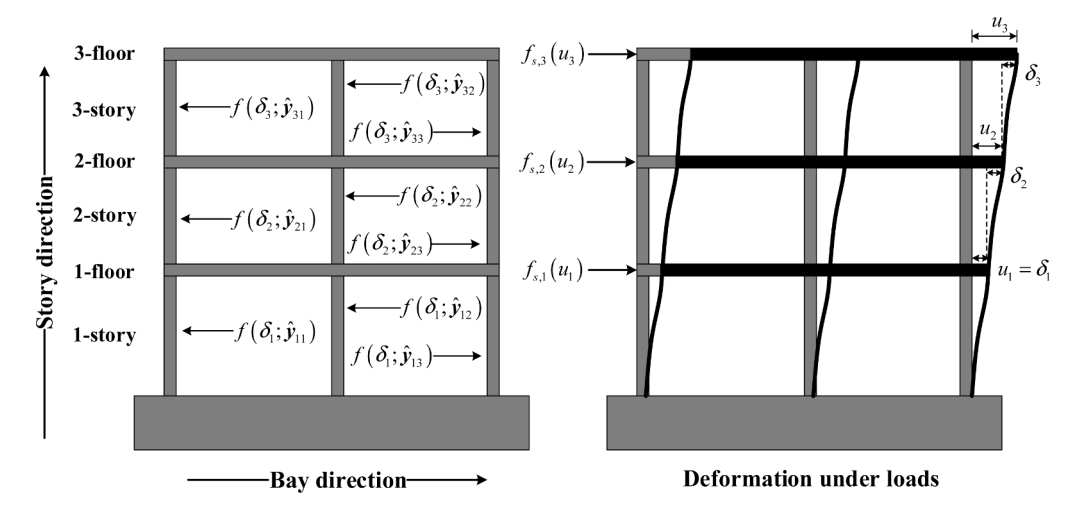


Fig. 1. Schematic representation of the proposed AI-enhanced shear building model.

mathematical formulation of the proposed approach is introduced in the following section.

#### 3. Methodology

This section presents the novel AI-enhanced computational method to accurately and efficiently predict the hysteretic behavior and timehistory response quantities of target RC frames subjected to both quasi-static cyclic loading and ground motions. The computational novelty of the proposed approach is that it can link the structural features with the experimental data by incorporating the AI technique with the well-established mechanical model (i.e., shear building model). To be specific, the AI technique can directly utilize the structural features and experimental force-displacement data of RC columns to determine the lateral stiffness of each column in the target RC frame while the structural stiffness matrix is efficiently formulated from the determined lateral stiffness of each column by means of the shear building model. Therefore, this scheme can capture the variation in structural response for a new RC frame with changes in structural features and enhance the prediction accuracy due to the use of real-world data while maintaining computational efficiency due to the incorporation of the shear building model. Additionally, two new data-driven seismic response solvers, one for quasi-static cyclic loading and one for dynamic ground motions, are developed to implement the proposed approach based on a database including 272 RC column specimens. More detailed information is introduced in the following sub-sections.

# 3.1. Artificial Intelligence (AI)-enhanced shear building model

The structural components in an RC frame mainly include beams and columns that are connected to form a frame system. When the frame is subjected to external loads, these components will deform along their DOFs (e.g., rotation and translation). It is very important to determine the stiffness for each component in deformation along its DOF since it will be used to form the structural stiffness matrix which in turn is used to calculate the force or deformation response at the system level. When the force is known (i.e., load-controlled analysis), the structural stiffness matrix is used to calculate the deformation caused by the applied force. When the displacement is known (i.e., displacement-controlled analysis), the structural stiffness matrix is instead used to calculate the force induced by the applied displacement. The method employed to formulate the structural stiffness matrix is an important factor to determine the computational efficiency and prediction performance. The detailed formulation of the proposed approach is presented in the following subsections. Briefly, Section 3.1.1 introduces the development of hysteretic modelers to define the nonlinear behavior of RC columns in an RC frame. Section 3.1.2 presents the formulation of an MDOF model for the RC frame based on the column hysteresis modelers presented in Section 3.1.1. Section 3.1.3 discusses tje data-driven solvers developed to obtain seismic response solutions for the MDOF model under quasi-static cyclic loading and dynamic ground motions.

#### 3.1.1. Development of hysteretic modelers for RC columns

In the formulation of the proposed method, the following assumptions are made to maintain consistency with the traditional shear building model: 1) axial deformations are ignored in all structural components; 2) masses for each story are idealized as lumped at the floor level; 3) all beams are rigid axially and in flexure such that only translational (horizontal) displacement is considered at each floor level. For the traditional shear building method, accurate definitions of the hysteretic constitutive relation (i.e., lateral force-deformation relation) for each story determine the predictive performance. However, there is still no unified and effective method to accurately define these constitutive relations based on the column features (e.g., column's design information). This poses a great shortcoming in the shear building model and prohibits full use of such a computationally efficient method. To solve this problem, we utilize real-world existing force-deformation data of RC columns subjected to cyclic loading and an AI technique to define the hysteretic constitutive relation (i.e., nonlinear behavior) of each column in each story. The hysteresis constitutive relation at the story level can then be defined via the hysteretic constitutive relations of all columns in the story as equivalent parallel springs. A schematic representation of the proposed AI-enhanced shear building model is presented in Fig. 1. As seen in Fig. 1, all columns in each story have the same story deformation (i.e., floor displacement) (e.g., the first story deformation  $\delta_1$  equals the deformation of each column in the first story) while the story shear (i.e., lateral force) can be obtained by summation of the lateral shear force for each column at the story deformation. This case is equivalent to the parallel springs since each column in each story can be regarded as a nonlinear spring. We denote the hysteretic constitutive relation of each column in each story by the hysteretic modeler  $[f_s, k] = f(\delta; y)$ , where  $y \in R^{n_{\theta}}$  is the optimal critical parameter vector containing  $n_{\theta}$  critical parameters that define a hysteretic model, and  $f(\bullet)$  represents the hysteretic model. This modeler is employed to produce the force  $f_s$  and lateral stiffness k for columns in an RC frame at a deformation  $\delta$  for each load step or time instant. The development of such a hysteretic modeler is based on an AI technique, a hysteretic model, and a training set [25].

Specifically, given the collected physical experimental data (i.e., structural features and force-deformation data) of n column specimens, a training set  $\{(x_i, y_i)\}_{i=1}^n$  consisting of the necessary structural features

(e.g., specimen geometry and material properties) denoted as  $x_i \in \mathbb{R}^p$ that serve as predictors and an optimal critical parameter vector  $y_i \in R^{n_\theta}$ that serves as the response variables can be developed. More detailed information regarding the development of the training set will be introduced in Section 4. Given the training set, a well-trained model for column performance prediction can be formed by learning the nonlinear relations exhibited by this data using the AI technique. The well-trained AI model is denoted as  $\hat{y} = M(x; \Psi)$ , where  $\hat{y}$  is the predicted critical parameter vector that defines a hysteretic model,  $\Psi \in \mathbb{R}^{n_{\psi}}$  is the optimal AI model parameter vector containing  $n_{\psi}$  parameters and  $M(\bullet)$  represents the AI technique. Since the response variable is continuous, only AI techniques related to regression can be used. Then, given an RC frame, each column in each story needs to be expressed as a query point denoted as  $x_{new} \in R^p$  that has the same structural features as  $x_i \in R^p$  in the training set. These query points for all columns in the RC frame are input to the well-trained AI model to obtain the predicted critical parameter vector  $\hat{y}_{new} = M(x_{new}; \Psi)$ . The predicted critical parameter vector  $\hat{y}_{new}$  is then applied to the hysteretic model to form the hysteretic modeler  $[f_s, k] = f(\delta; \hat{y}_{new})$ . Luo and Paal [25] developed a method to form the component-level hysteretic modeler, and the performance of this method has been successfully validated for nonlinear seismic response prediction of circular RC columns subjected to quasi-static cyclic loading and dynamic earthquake ground motions. In this paper, the method presented in Luo and Paal [25] is utilized to develop the component-level hysteretic modelers for all RC columns in an RC frame. It should be noted that the difference between the work presented in this paper and the one in Luo and Paal [25] is significant. First, the work in Luo and Paal [25] mainly introduces the integration of an AI technique and hysteretic model for nonlinear seismic response prediction of structural components, while the study in this paper presents the integration of an AI technique, hysteretic model, and system-level mechanical model (i.e., shear building model) for nonlinear seismic response prediction of structural systems. Therefore, the method and corresponding data-driven solver in Luo and Paal [25] are only applicable for the single-degree-of-freedom (SDOF) case and cannot be used for the MDOF case. Second, the database for the two approaches is different. The database utilized to develop the component-level hysteretic modeler for Luo and Paal [25] includes 154 circular sectional colthe columns in the i-th story have the same lateral translational DOF. Thus, the total mass for the i-th story is  $\sum_{j=1}^{l+1} m_{ij}$  (note: beam and slab masses have been considered in the column's self-weight), and the mass matrix for this structure is diagonal in the lateral DOF direction, which is written as follows:

$$\mathbf{M} = \begin{bmatrix} \sum_{j=1}^{l+1} m_{1j} & 0 & 0 \\ 0 & \ddots & 0 \\ 0 & 0 & \sum_{j=1}^{l+1} m_{nj} \end{bmatrix}$$
 (1)

The mass matrix will remain constant throughout the response history. As shown in Fig. 1, the hysteretic parameters (e.g., lateral stiffness or lateral force) for each column in each story is obtained by the hysteretic modeler developed in this work and presented in Section 3.1.1, which is denoted as  $\left[f_{s,ij},k_{ij}\right]=f\left(\delta_{i};\widehat{\mathbf{y}}_{ij}\right)$  where  $f_{s,ij}$  and  $k_{ij}$  are the lateral force and lateral stiffness of column j located at story i and obtained by the modeler  $f\left(\delta_i; \widehat{\mathbf{y}}_{ij}\right)$  given the  $i^{th}$ -story relative displacement (or story drift)  $\delta_i$ , respectively (note: lateral force is a general term that represents the force  $f_{s,ij}$  induced by a lateral deformation  $\delta_i$  applied to a structure system, and it could be peak force or yield force, depending on the magnitude of the lateral deformation  $\delta_i$ ). The calculation of  $\delta_i$  is  $\delta_i =$  $u_i - u_{i-1}$ ,  $i \ge 2$ , and when i = 1,  $\delta_1 = u_1$ , which means that the relative story displacement  $\delta_1$  is equal to the lateral displacement  $u_1$  at the first floor, where  $u_i$  is the lateral displacement relative to the ground at floor i. Note that the hysteretic parameters for each column in each story could be the same or they could vary from one another, depending on the obtained optimal critical parameter vector  $\widehat{\boldsymbol{y}}_{ij}.$  Since the columns in each story can be considered equivalent to springs in parallel, each story stiffness can be obtained by summation of the obtained lateral stiffness for each column in the story (e.g., the  $i^{th}$ -story stiffness is  $\sum_{i=1}^{l+1} k_{ij}$ ). Due to the assumptions made in Section 3.1.1, the structural stiffness matrix can be formulated and is a symmetric tridiagonal matrix, which is written as follows:

$$\mathbf{K} = \begin{bmatrix}
\sum_{j=1}^{l+1} (k_{1j} + k_{2j}) & -\sum_{j=1}^{l+1} k_{2j} & 0 & \cdots & 0 \\
-\sum_{j=1}^{l+1} k_{2j} & \sum_{j=1}^{l+1} (k_{2j} + k_{3j}) & -\sum_{j=1}^{l+1} k_{3j} & \ddots & \vdots \\
0 & -\sum_{j=1}^{l+1} k_{3j} & \sum_{j=1}^{l+1} (k_{3j} + k_{4j}) & \ddots & 0 \\
\vdots & \ddots & \ddots & -\sum_{j=1}^{l+1} k_{nj} \\
0 & \cdots & 0 & -\sum_{j=1}^{l+1} k_{nj} & \sum_{j=1}^{l+1} k_{nj}
\end{bmatrix}$$
(2)

umn specimens, while this study includes 272 rectangular sectional column specimens.

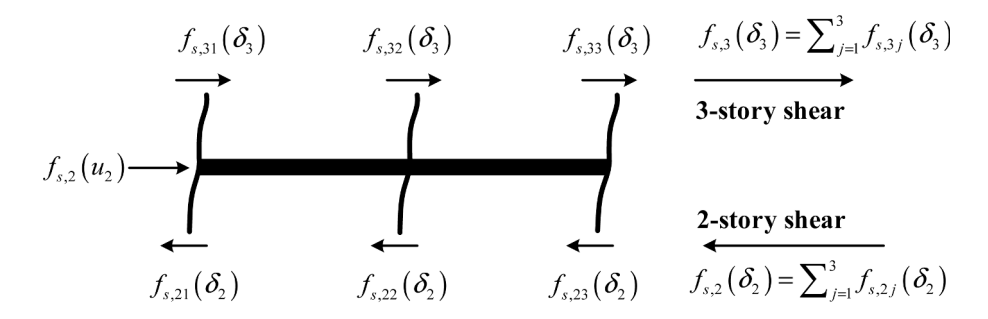
# 3.1.2. Formulation of an MDOF model

Assume a planar RC frame structure that has n-stories, with each story having l-bays, as shown in Fig. 1 in the case of n=3 and l=2. Based on the aforementioned assumptions, each column in the i-th story has a self-weight, denoted as  $m_{ij}$ , where  $i=1,\cdots,n$ , represents the story, and  $j=1,\cdots,l+1$  represents the column along the bay direction, and all

The structural stiffness matrix K will be updated when the column lateral stiffness  $k_{ij}$  changes due to nonlinear behavior throughout the response history. For the damping component, Rayleigh damping is used, which is a combination of mass-proportional and stiffness-proportional damping. The Rayleigh damping matrix is written as follows:

$$C = a_0 \mathbf{M} + a_1 \mathbf{K} \tag{3}$$

The coefficients  $a_0$  and  $a_1$  can be determined from specified damping



Static equilibrium:  $f_{s,3}(\delta_3) + f_{s,2}(u_2) = f_{s,2}(\delta_2)$ 

Fig. 2. Determination of the resisting force from story shear by static equilibrium.

ratios  $\zeta_{i_m}$  and  $\zeta_{j_m}$  for the  $i_m$  <sup>th</sup> and  $j_m$  <sup>th</sup> modes, respectively. The detailed information regarding the calculation of  $a_0$  and  $a_1$  can be found in Chopra [5]. Given the mass, stiffness, and damping components, an MDOF model for an RC frame structure subjected to ground motions can be formulated.

$$M\ddot{u} + C\dot{u} + f_S(u) = -M1\ddot{u}_g(t) \tag{4}$$

where  $u=(u_1,u_2,\cdots,u_n)^T$  is a displacement vector along the structure's height, and each element represents the lateral floor displacement relative to the ground;  $f_S(u)$  is a lateral resisting force vector along the structure's height determined by the structural stiffness matrix K and corresponding displacement vector u, or directly assembled by the story shear force  $\sum_{j=1}^{l+1} f_{s,ij}$ ,  $i=1,\cdots,n; 1=(1,\cdots,1)\in R^n$  is an influence vector that represents the fact that the proposed MDOF model has all dynamic DOFs in the direction of the ground motion [5]; and,  $\ddot{u}_g(t)$  is the ground motion.

Note that Eq. (4) can be applied to both linear and nonlinear systems. This is because when solving Eq. (4), the structural stiffness matrix K is not constant and will be updated to determine the resisting force vector  $f_S(u)$  from the column lateral stiffness corresponding to the deformation and state of each column. The data-driven solvers developed to obtain the hysteretic behavior and time-history response quantities will be introduced in the following sub-section.

# 3.1.3. Development of data-driven solvers for seismic response prediction

For the linear analysis, the initial structure stiffness matrix is used throughout the entire time history. Therefore, the  $f_S(u)$  term in Eq. (4) can be changed to Ku where K represents the initial structure stiffness matrix and will remain constant. For the nonlinear analysis, the structural stiffness matrix K is not constant and will be updated to determine  $f_{\rm c}(u)$  from the column lateral stiffness corresponding to the deformation and state of each column in each story. Specifically, given the relative story displacement  $\delta_i$  and state (e.g., loading or unloading) of each column in each story, the column hysteretic modelers can adaptively produce the lateral force and lateral stiffness  $\left[f_{s,ij},k_{ij}\right]=f\left(\delta_i;\widehat{y}_{ij}\right)$  and record the current state. The recorded current state determines if the deformation is in the loading branch, unloading branch, or at the reversal point where a transition happens between loading and unloading and thus can inform the hysteretic modelers to determine the lateral force and lateral stiffness for the next load step or time instant. The produced lateral force  $f_{s,ij}$  and lateral stiffness  $k_{ij}$  for each column can be respectively assembled to a resisting force vector  $f_S(u)$  and structural stiffness matrix K for further calculation. Eq. (2) can be used to assemble a structural stiffness matrix K from the column lateral stiffness  $k_{ii}$  produced by the column hysteretic modelers. Since the forcedisplacement relation is nonlinear, the direct calculation of the resisting force vector by  $f_S(u) = Ku$  is no longer valid. The static equilibrium

constraint is used to directly assemble the resisting force vector  $f_S(u)$  from the column shear force  $f_{s,ij}(\delta_i)$  obtained by the column hysteretic modelers,  $i=1,\cdots,n; j=1,\cdots,l+1$ , . Fig. 2 displays an example to illustrate how the resisting force  $f_{s,2}(u_2)$  at the 2nd floor is formed using the static equilibrium constraint.

Specifically, given the shear force  $f_{s,ij}(\delta_i)$  for each column at story i, the  $i^{th}$ -story shear force can be calculated as  $f_{s,i}(\delta_i) = \sum_{j=1}^{l+1} f_{s,ij}(\delta_i)$ . The resisting force vector  $f_S(u)$  consists of the resisting force  $f_{s,i}(u_i)$  at each floor, which is denoted as  $f_S(u) = \left(f_{s,1}(u_1), f_{s,2}(u_2) \cdots, f_{s,n}(u_n)\right)^T$ . The resisting force  $f_{s,i}(u_i)$  at floor i is made up of two components:  $f_{s,i}(\delta_i)$  from the story of floor i below, and  $f_{s,i+1}(\delta_{i+1})$  from the story of floor i above, as shown in Fig. 2. To maintain static equilibrium, the following equation can be established:

$$f_{s,i+1}(\delta_{i+1}) + f_{s,i}(u_i) = f_{s,i}(\delta_i), 1 \le i \le n-1$$
(5)

When i=n, the resisting force  $f_{s,n}(u_n)$  equals  $f_{s,n}(\delta_n)$ . This is because there is no story above floor n. So, the resisting force vector  $f_s(u)$  can be re-written as follows:

$$f_{S}(\mathbf{u}) = (f_{s,1}(\delta_{1}) - f_{s,2}(\delta_{2}), \dots, f_{s,n-1}(\delta_{n-1}) - f_{s,n}(\delta_{n}), f_{s,n}(\delta_{n}))^{T}$$
(6)

Thus, Eq. (6) can be used to assemble a resisting force vector  $f_S(u)$  from each column shear force in each story, which will be updated for each time instant. For the displacement-controlled quasi-static cyclic loading, the floor displacement information u is known, and the quantity of interest is regarding the hysteretic relationship between base shear and roof displacement or story shear and story drift (i.e., relative story displacement). The prediction of these quantities using the proposed AI-enhanced shear building model is straightforward. Given an RC column training set  $\{(x_i, y_i)\}_{i=1}^n$ , the following procedure, serving as a data-driven solver, is developed to implement the proposed approach for predicting the hysteretic response of an RC frame subjected to quasi-static cyclic loading.

Algorithm 1: Implementation of proposed AI-enhanced MDOF model under quasistatic cyclic loading

- (b) train an AI model  $M(x; \Psi)$  based on the RC column training set  $\{(x_i, y_i)\}_{i=1}^n$ ;
- (c) predict the response for each column in the target RC frame, denoted as  $\hat{y}_{ij} = M(x_{\text{new},ij}; \Psi)$ ;
- (d) form a hysteretic modeler for each column, denoted as  $\left[f_{s,ij},k_{ij}\right]=f\left(\delta_i;\widehat{\mathbf{y}}_{ij}\right), i=1,$  ..., $r_i:j=1,...,l+1;$
- ${\bf 2.}\ {\bf Predict}\ {\bf hysteretic}\ {\bf response}\ {\bf using}\ {\bf proposed}\ {\bf AI-enhanced}\ {\bf MDOF}\ {\bf model};$

(continued on next page)

<sup>1.</sup> Development of hysteretic modelers:

Given an RC column training set  $\{(x_i, y_i)\}_{i=1}^n$  and a target RC frame with n stories and l

<sup>(</sup>a) translate the columns in each story in the target RC frame into predictors, denoted as query points  $\{(\mathbf{x}_{\text{new},ij})\}_{i,j=1}^{n\times(l+1)};$ 

#### (continued)

Algorithm 1: Implementation of proposed AI-enhanced MDOF model under quasistatic cyclic loading

```
Given the displacement history U = (u^1, \dots, u^D)^T, hysteretic modeler f_{s,ij}, k_{ij} = 0
   f(\delta_i; \widehat{\mathbf{y}}_{ij}), i = 1,...,n; j = 1,...,l+1
for d = 1 to D do
  for i = 1 to n do
      (a) when i=1, calculate the relative story displacement or story drift \delta_1^d=u_1^d
      (b) when i \neq 1, calculate the relative story displacement or story drift \delta_i^d =
   u_i^d - u_{i-1}^d
      for j = 1 to l + 1 do
         (a) calculate the shear and lateral stiffness \left[f_{s,ij}(\delta_i^d), k_{ij}(\delta_i^d)\right] = f\left(\delta_i^d; \hat{y}_{ij}\right) for
   each column;
      end for j
      (a) calculate and record the story shear f_{s,i}(\delta_i^d) = \sum_{i=1}^{l+1} f_{s,ii}(\delta_i^d);
      (b) calculate and record the story stiffness k_i(\delta_i^d) = \sum_{i=1}^{l+1} k_{ij}(\delta_i^d);
   (a) assemble the structure stiffness matrix K^d according to \{(k_i(\delta^d_i))\}_{i=1}^n using Eq.
  (2):
   (b) assemble the resisting force vector f_S(u^d) according to \left\{ \left( f_{s,i}(\delta_i^d) \right) \right\}_{i=1}^n using Eq.
   (c) output \left\{ \left( f_{s,i}(\delta_i^d) \right) \right\}_{i=1}^n, f_S(u^d), and K^d.
End for d
```

By implementing Algorithm 1 presented above, one can obtain the hysteretic response of both roof displacement  $(\{(u_n^d)\}_{d=1}^D)$  versus base shear ( $\left\{\left(f_{s,1}\left(\delta_{1}^{t}\right)\right)\right\}_{d=1}^{D}$ ) and story drift ( $\left\{\left(\delta_{i}^{d}\right)\right\}_{d=1}^{D}$ ) versus story shear  $(\left\{\left(f_{s,i}(\delta_i^d)\right)\right\}_{d=1}^D)$  for a target RC frame structure. Further, Algorithm 1 can also output the structural stiffness matrix  $\left\{\left(\mathbf{\textit{K}}^d\right)\right\}_{d=1}^D$  and resisting force vector  $\{(f_S(u^d))\}_{d=1}^D$  given the entire displacement history U= $(u^1, \dots, u^D)^T$ , which are important components for the nonlinear timehistory analysis. Thus, Algorithm 1 will be used in Algorithm 2 below to calculate the structural stiffness matrix K and resisting force vector  $f_s(u)$  given the displacement information u, which is denoted as  $[f_s(u)]$ , K = Algorithm1(u). The nonlinear dynamic analysis involves solving the equations of motion presented in Eq. (4), which requires a numerical method to solve the nonlinear system. In this paper, a hybrid algorithm coupling the Newmark average acceleration (NAA) method, modified Newton-Raphson (MNR) iteration, and Algorithm 1 is developed to solve Eq. (4). The detailed procedure is presented below.

Algorithm 2: Implementation of proposed AI-enhanced MDOF model under dynamic ground motions

```
Given the ground motion \left\{\left(\ddot{u}_{\mathbf{g}}(t_{\mathbf{f}})\right)\right\}_{t=1}^{T}, hysteretic modeler \left[f_{\mathbf{s},ij},k_{ij}\right]=f\left(\delta_{i};\widehat{\mathbf{y}}_{ij}\right),i
     =1,...,n; j=1,...,l+1;
```

- (a) calculate the nodal mass  $m_{ij}$  in each story for the target RC frame;
- (b) calculate the initial lateral stiffness for each column from the hysteretic modeler:  $\left|f_{s,ij},k_{ij}\right|=f\left(\delta_{i};\widehat{y}_{ij}\right);$
- (c) calculate the mass, initial stiffness, and damping matrix M,  $K^0$ , and C using Eqs. (1-3), respectively;
- (d) select an appropriate time interval  $\Delta t$  and calculate the earthquake forces:  $p^t =$  $-M1\ddot{u}_{\sigma}(t_{t});$
- (e) calculate the Newmark coefficients:  $A = 4M/\Delta t + 2C$ ; B = 2M;
- 2. Solving Eq. (4) by the hybrid algorithm:
- Given the initial condition of the target RC frame, i.e.,  $p^0$ ,  $u^0$ , and  $\dot{u}^0$ ,  $f_S(u^0)$ , and known information from step 1:
- (a) calculate the  $\ddot{u}^0 = M^{-1} (p^0 C\dot{u}^0 f_S(u^0));$

# $\mathbf{for}\ t = 1\ \mathbf{to}\ T\ \mathbf{do}$

- (a)  $\Delta \hat{p}^{t-1} = p^t p^{t-1} + A\dot{u}^{t-1} + B\ddot{u}^{t-1};$ (b)  $\hat{K}^{t-1} = K^{t-1} + 2C/\Delta t + 4M/(\Delta t)^2;$
- (c) calculate the  $\Delta u^{t-1}$ ,  $K^t$ ,  $f_s(u^t)$  using modified Newton-Raphson and algorithm 1

(continued on next column)

#### (continued)

Algorithm 2: Implementation of proposed AI-enhanced MDOF model under dynamic ground motions

```
Given f_s(u^{t-1}), u^{t-1}; \Delta \hat{p}^{t-1}, \hat{K}^{t-1}, K^{t-1}, the maximum number of iteration N, and
        (a) initial assignment: f_s(u_0^t) = f_s(u^{t-1}), u_0^t = u^{t-1}, \Delta R_1 = \Delta \widehat{p}^{t-1}, \widehat{K} = \widehat{K}^{t-1},
   K = K^{t-1};
        for j_n = 1 to N do
            (a) \Delta u_{j_n} = \widehat{K}^{-1} \Delta R_{j_n};
            (b) u_{j_n}^t = u_{j_n-1}^t + \Delta u_{j_n};
            (c) calculate the K_{i_n}^t and f_s(u_{i_n}^t) using the algorithm 1: [f_s(u_{i_n}^t), K_{i_n}^t] =
            (d) \Delta f_{j_n} = f_s \left( u_{j_n}^t \right) - f_s \left( u_{j_n-1}^t \right) + (\widehat{K} - K) \Delta u_{j_n};

(e) \Delta R_{j_n+1} = \Delta R_{j_n} - \Delta f_{j_n};
            (f) calculate the displacement convergence criterion: \Delta u = \sum_{i=1}^{j_n} \Delta u_{i_n}, eps =
            (h) \Delta u^{t-1} = \Delta u, K^t = K_{i_*}^t, and f_s(u^t) = f_s(u_{i_*}^t);
            if eps \le tol do
                (a) break the loop;
            end if
        end for j_n
    (d) \Delta \dot{\boldsymbol{u}}^{t-1} = 2\Delta \boldsymbol{u}^{t-1}/\Delta t - 2\dot{\boldsymbol{u}}^{t-1};
    (e) \Delta \ddot{u}^{t-1} = 4\Delta u^{t-1}/(\Delta t)^2 - 4\dot{u}^{t-1}/\Delta t - 2\ddot{u}^{t-1};
   (f) u^t = u^{t-1} + \Delta u^{t-1}, \dot{u}^t = \dot{u}^{t-1} + \Delta \dot{u}^{t-1}, and \ddot{u}^t = \ddot{u}^{t-1} + \Delta \ddot{u}^{t-1};
end for t
```

By implementing Algorithm 2, the time-history response quantities of interest, such as time versus roof displacement and the distribution of peak story drift ratio along the floors can be obtained. It should be noted that the displacement convergence criterion in Algorithm 2 for the proposed AI-enhanced shear building model is satisfactory since the numerical values in the displacement vector have the same units (i.e., lateral displacement) and do not suffer the complications associated with different units that bring in significant errors [5]. For algorithms 1 and 2, the locally weighted least-squares support vector machines for regression (LWLS-SVMR) [22] is selected as the AI technique. LWLS-SVMR is a local machine learning (ML) model which was recently developed for the generalized prediction of the drift capacity of RC columns [22]. LWLS-SVMR integrates LS-SVMR [43] with a locally weighted learning algorithm to locally adjust the capacity of LS-SVMR to the properties of the training set in each area of the input space, thus enhancing the generalization performance of the LS-SVMR. One main advantage of LWLS-SVMR is that it only requires the fitting of a subset of training data nearby (relevant to) the query point while existing global ML methods require fitting the entire set of training data. In this sense, the LWLS-SVMR can avoid the potential negative influence of irrelevant points, achieving a suitable trade-off between the capacity of the learning system and the number of training data points.

# 4. Rectangular column database

For this study, a database of rectangular RC column experimental tests is used to evaluate the performance of the novel AI-enhanced shear building model in predicting the seismic response of RC frames under both displacement-controlled quasi-static cyclic loading and dynamic ground motions. The database is taken from the authors' previous work [21]. The original number of column specimens in the dataset is 262, which is primarily based on the database compiled by Berry et al. [2]. However, there are ten columns for which the force-displacement data are not available. These ten columns are from Verderame et al. [46] and Eom et al. [9] and thus, are not included in this work. Additionally, as the shake table tests for large-scale RC frames with several stories and bays (e.g., RC frame with more than 6 stories and 2 bays) are not available, the shake table tests for small-scale RC frames will be used. Since small-scale RC frames have column features outside the range of

the dataset, the dataset is supplemented with 20 small-scale RC column specimens to reduce potential sample bias. These column specimens are taken from Cecen [4]. Thus, the final number of column specimens in the dataset is 272.

For the development of the training set  $\{(x_i, y_i)\}_{i=1}^{272}$ , the predictor variables  $x_i$  and response variables  $y_i$  are required to be extracted from the collected column data. For each column specimen in the database, the predictor variables  $x_i$  are extracted from the structural features (i.e., design information) including the gross column cross-sectional area  $A_g$ , concrete compressive strength  $f_c$ , longitudinal reinforcement yield stress  $f_{vl}$ , longitudinal reinforcement area  $A_{sl}$ , column effective depth d, concrete cover c, transverse reinforcement yield stress  $f_{yt}$ , transverse reinforcement area  $A_{st}$ , stirrup spacing s, shear span a, and applied axial load P. The response variables  $y_i$  are extracted from experimentally recorded force-deformation data including the monotonic backbone curve and hysteretic parameters via the hysteretic model and optimization algorithm. In this paper, the modified three-parameter hysteretic model and the hybrid optimization algorithm proposed in Luo and Paal [25] are utilized to extract the three hysteretic parameters (i.e., stiffness deterioration parameter  $\alpha$ , strength deterioration parameter  $\beta$ , and pinching parameter  $\gamma$ ) from each column's force-deformation data. Since the monotonic backbone curve parameters cannot be directly extracted from cyclic force-deformation data, they are approximated via cyclic backbone curve parameters that are extracted using the methods presented in Sezen and Moehle [40] and Elwood and Moehle [8]. As the forces and displacements in the positive and negative directions in the experimental hysteretic curve are near-identical, the cyclic backbone curve parameters in the positive and negative directions are designated as equivalent in this work, as shown in Fig. 3.

Finally, nine optimal critical parameters, including six cyclic backbone curve parameters and three hysteretic parameters, for each of the 272 columns in the database are obtained according to the method proposed in Luo and Paal [25]. Note that the cyclic backbone curve parameters need to be transformed to the monotonic backbone curve parameters when developing the hysteretic modeler. The transformation from the cyclic backbone curve to the monotonic backbone curve can be found in Luo and Paal [25]. The statistical properties of the optimal cyclic backbone curve and three hysteretic parameters for the 272 column specimens are summarized in Table 1.

Table 1
Statistical properties of the optimal cyclic backbone curve and hysteretic parameters

purumeters.					
Critical Parameters	Minimum	Maximum	Median	Sample Mean	Std. Dev
Yield shear force, V <sub>y</sub> (kN)	1.60	1071.01	130.50	163.72	149.05
Drift ratio at yield shear, $\delta_y$ (%)	0.20	1.73	0.79	0.85	0.37
Maximum shear force, $V_m$ (kN)	1.84	1338.80	155.09	194.63	178.50
Drift ratio at maximum shear, $\delta_m$ (%)	0.31	7.94	1.69	1.99	1.33
Ultimate shear force, $V_u$ (kN)	1.64	1217.01	126.89	163.03	155.51
Drift ratio at ultimate shear, $\delta_u$ (%)	0.72	9.39	3.15	3.60	1.88
Stiffness deterioration parameter, $\alpha$	0.30	119.42	9.37	21.09	21.98
Strength deterioration parameter, β	0.00	0.93	0.06	0.14	0.20
Pinching parameter,γ	0.31	1.00	0.98	0.87	0.19

# 5. Numerical experiments and discussion of results

This section presents the numerical experiments carried out to validate the proposed AI-enhanced method in accurate and efficient seismic response prediction of RC frame structures under quasi-static cyclic loading and dynamic earthquake ground motions. For the quasi-static cyclic loading case, a large-scale (1:2) physical experimental model of a 3-bay, 3-story RC frame structure is selected from Xie et al. [50] to serve as the test specimen. For the dynamic earthquake ground motion case, two small-scale (1:15) physical experimental models of 3-bay, 9story RC frame structures, one subjected to four earthquake (EQ) ground motions and another subjected to six EQ ground motions are selected from Schultz [39] to serve as the test specimens. For both cases, the whole rectangular column dataset presented in Section 4 is used to train the proposed method, and the proposed approach is compared with the widely used fiber-based modeling method with experimental data serving as the ground truth. All the numerical experiments are performed using a Desktop PC with the Processor: Intel® Xeon® CPU E3-

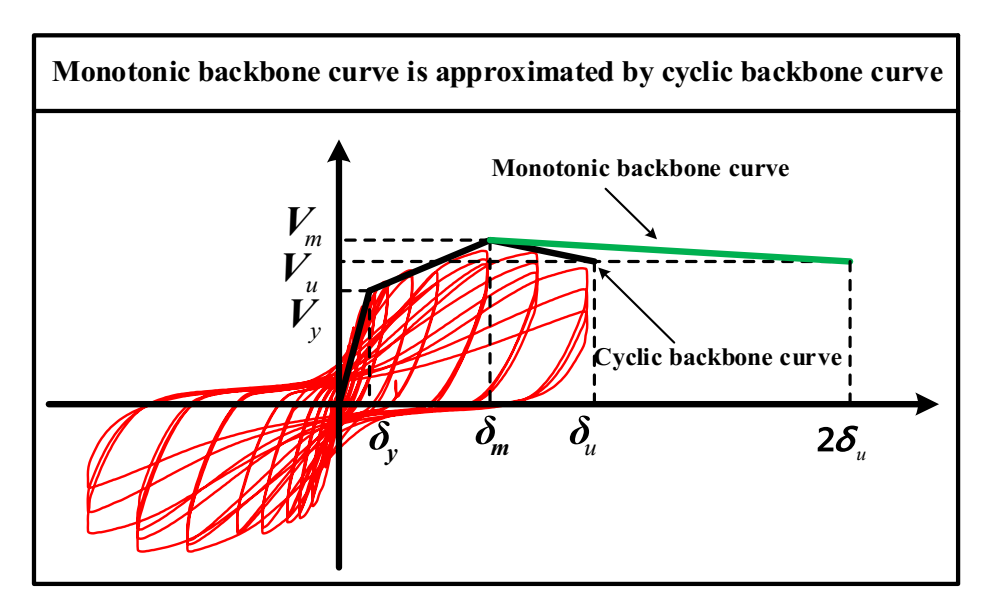


Fig. 3. Schematic for approximating the monotonic backbone curve via the cyclic backbone curve.

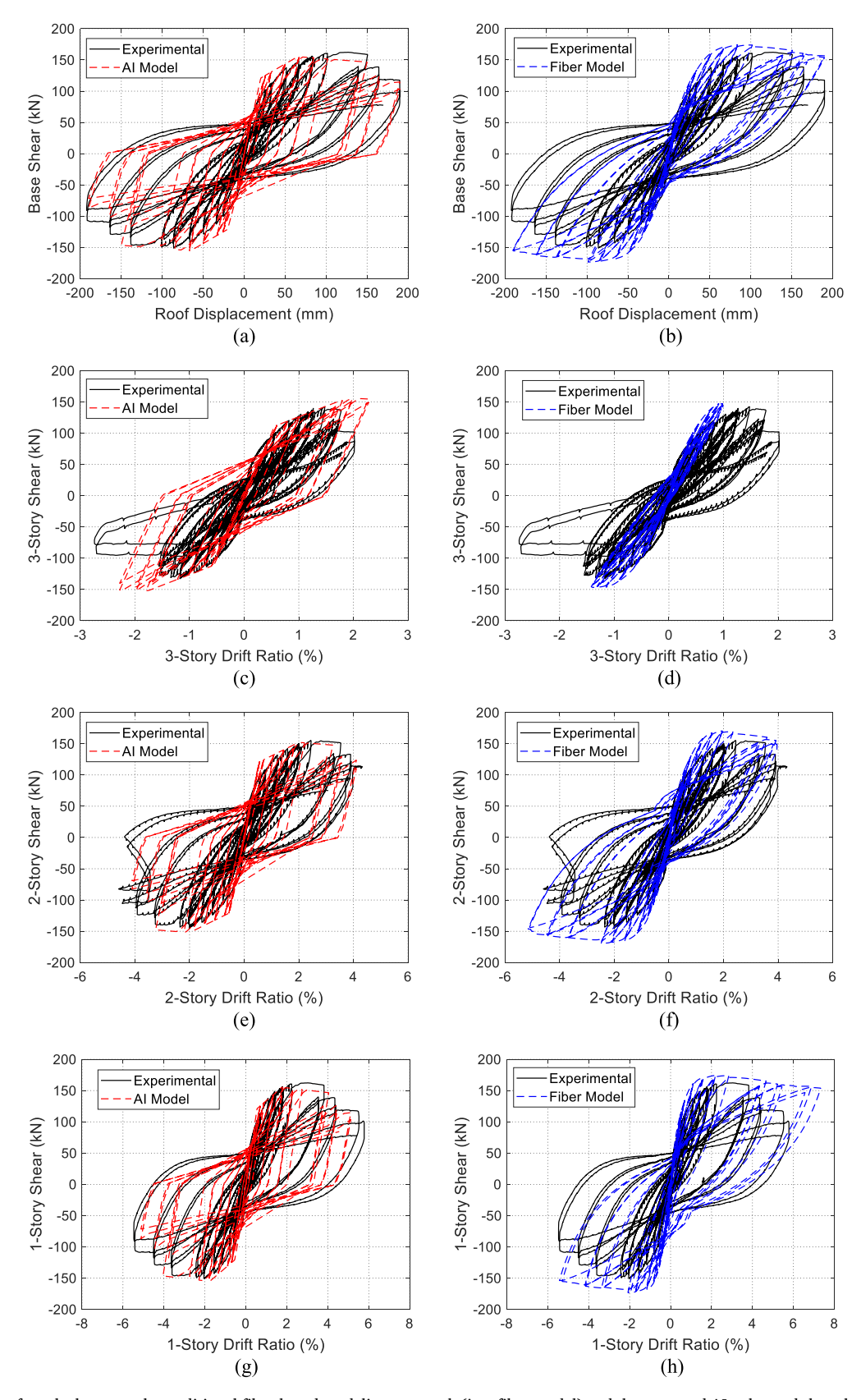


Fig. 4. Comparison of results between the traditional fiber-based modeling approach (i.e., fiber model) and the proposed AI-enhanced shear building model (i.e., AI model), with the experimental data serving as the ground truth.

**Table 2** Performance comparison between the proposed approach and fiber-based method in terms of error rate (%) that is computed by  $|Q_p - Q_e| \times 100/Q_e$ , where  $Q_p$  is the predicted quantity and  $Q_e$  is the experimentally observed quantity. Bold values represent the best performance.

Model	Structure	Yield Force	Peak Force	Drift Capacity	Energy Dissipation
Proposed Approach	Story 1	4.44	4.41	1.42	12.95
**	Story 2	8.56	2.28	3.34	3.03
	Story 3	6.17	9.06	31.17	11.61
	Integrated frame	1.82	4.41	0.36	1.67
Fiber-based approach	Story 1	10.56	7.29	68.10	18.44
**	Story 2	23.17	9.71	1.59	16.48
	Story 3	11.62	3.39	43.01	64.01
	Integrated frame	14.11	7.29	15.55	4.37

 $1270\ v6\ @\ 3.80\ GHz$  and the max memory size that is 64 GB. No parallel computing is employed for any of the numerical experiments.

# 5.1. Displacement-controlled quasi-static cyclic loading test

This section presents a comparison between the proposed AIenhanced method and the widely used fiber model to demonstrate the real-world application and full potential of the proposed approach. A large-scale (1:2) physical experiment of a 3-bay, 3-story RC frame subjected to displacement-controlled quasi-static cyclic loading is selected from Xie et al. [50] for this comparison. The lateral load distribution for this experimental test is an inverse triangle, and the entire loading process is controlled by the displacement of the top floor (i.e., roof displacement) [50]. The detailed information regarding the structural geometry, material properties, reinforcement details, and load pattern can be found in Xie et al. [50]. For the widely used fiber model, a single force-based fiber beam-column element [41,42] with five Gauss-Lobatto integration points (i.e., monitoring sections) is employed to model each of the columns and beams in the selected RC frame. In each monitoring section, the cover concrete fiber is simulated using the modified Kent and Park model [38], and the core concrete fiber is simulated by the confined concrete model proposed by Mander et al. [26] to represent the confinement effect of the stirrups. The reinforcement fiber is modeled by the Menegotto-Pinto model [31]. All the values that need to input these material constitutive models are selected based on the material properties from experimental information. OpenSees [30] is used to implement the RC frame numerical model established by the widely-used

fiber-based method to obtain the nonlinear response of the RC frame. Algorithm 1 presented in Section 3.1.3 is used to implement the proposed approach using Matlab 2018a to obtain the hysteretic responses of roof displacement versus base shear and story drift ratio versus story shear. It should be noted that the story drift ratio depends on the floor displacement, which depends on the roof displacement and mode shape. This is because an MDOF system's deformation shape depends on its modes of vibration [5]. Typically, each mode is normalized so that its largest element is unity (e.g., the top floor of a multistory building is unity). Therefore, if the roof displacement and mode shape are known, then all floor displacements can be obtained. As introduced above, the roof displacement is pre-defined by the experimental test, and thus the roof displacements for both proposed and fiber-based methods are the same. However, the mode shapes obtained by the proposed and fiberbased methods may vary due to the difference in stiffness. This will lead to the difference in story drift ratios obtained by the two methods.

Fig. 4 presents a comparison of the results between the proposed method (i.e., AI model (red dashed line)) and fiber-based modeling approach (i.e., fiber model (blue dashed line)) where ground truth is defined as the experimental test (solid black line). Fig. 4(a-b) demonstrates that both methods reasonably capture the global nonlinear response of the RC frame in terms of the hysteretic relation of roof displacement versus base shear. The proposed approach effectively reflects the cyclic strength deteriorations and softening behavior observed experimentally, while the fiber model fails to reasonably capture these types of hysteretic behavior. Thus, although both methods reasonably predict the overall hysteretic response, the proposed approach achieves better prediction capability than the fiber model, where the hysteretic curve predicted by the proposed approach has better agreement with the experimental results than that simulated by the fiber model. The hysteretic response of story drift ratio versus story shear is extracted and presented in Fig. 4(c-h). Both methods reasonably predict the lateral capacity of the RC frame, where the lateral strengths (i.e., maximum shear force) predicted by both methods are close to those observed experimentally. However, the fiber model still does not reasonably capture the softening behavior induced by cyclic strength deterioration, while the proposed approach can effectively reflect these types of behavior characteristics observed experimentally. In total, the proposed approach can reasonably reflect the hysteretic behavior of the RC frame, where the hysteretic curves for each story predicted by the proposed approach have reasonable agreement with experimental results as shown in Fig. 4(c,e,g). The story behaviors predicted by the fiber model show some discrepancy with the experimental results, as shown in Fig. 4 (d,f,h).

Table 2 presents the detailed performance comparison between the proposed approach and fiber-based method in terms of response

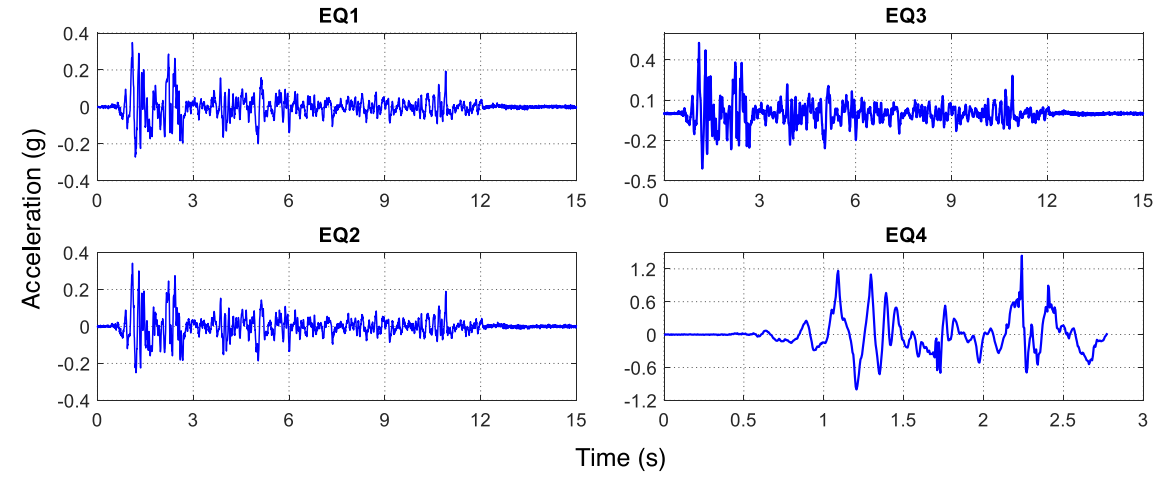


Fig. 5. Four time versus ground acceleration records for frame SS1.

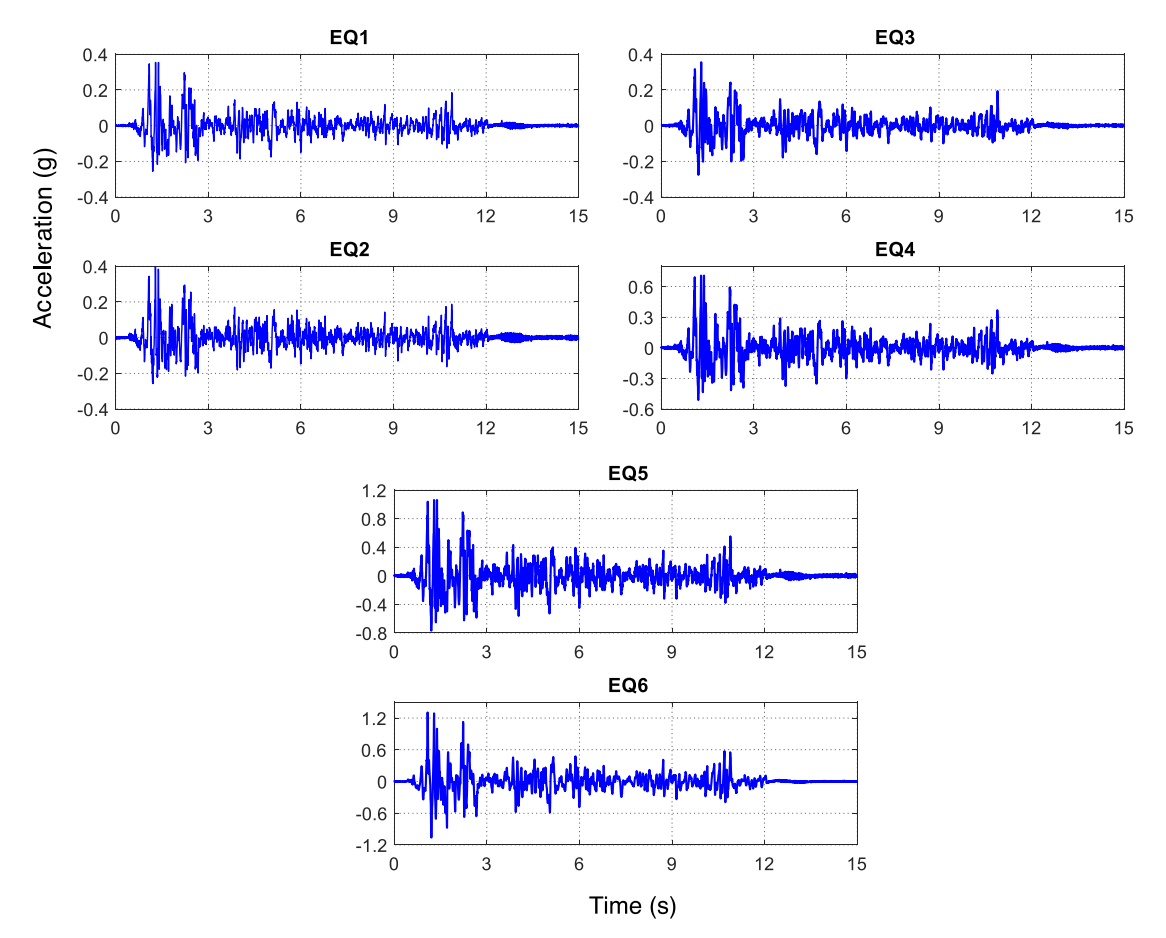


Fig. 6. Six time versus ground acceleration records for frame SS2.

quantities including yield force, peak force, drift capacity, and energy dissipation. The performance is quantified by error rate (%), which is computed by  $|Q_p - Q_e| \times 100/Q_e$ , where  $Q_p$  is the predicted response quantity and  $Q_e$  is the experimentally observed response quantity. As shown in Table 2, the proposed approach can more accurately predict all response quantities when compared to the fiber-based method across all stories. Furthermore, perhaps most importantly, predicting the hysteretic curve of the selected RC frame using the proposed method only takes 10 s, while using the traditional fiber model takes 1,672 s (or roughly 30 min). Therefore, the proposed approach significantly reduces the computational cost. Based on these comparisons, the proposed approach presented in this paper performs better than the traditional fiber-based modeling method. Thus, it is deemed that the proposed approach could be an appropriate and promising means for accurate and efficient seismic response prediction of RC frames subjected to reversed cyclic loading, especially for application in near-real-time scenarios.

# 5.2. Dynamic shake table tests

To validate the performance of the proposed approach in predicting the seismic response of RC frames subjected to ground motions, two small-scale (1:15), 3-bay, 9-story RC frame specimens are used as illustrative examples. Structure SS1 is subjected to four consecutive unidirectional ground motions (Fig. 5), and structure SS2 is subjected to six consecutive unidirectional ground motions (Fig. 6). These shake table tests were organized by Schultz [39], and the difference between these two test specimens is that the columns in frame SS2 have a higher longitudinal reinforcement ratio than those in frame SS1. Therefore, the columns in frame SS2 are stiffer than those in frame SS1. Detailed information regarding the physical experimental set-up, structural

features, ground motions, and shake table test results can be found in Schultz [39].

For the traditional fiber-based modeling approach, the fiber beamcolumn element is also used to model the seismic response of the two small-scale RC frames. The element type, integration method, number of integration points, material constitutive models described in Section 5.1 for the large-scale RC frame are also used here to establish the numerical models of the two RC frames. For the proposed approach, Algorithm 2 presented in Section 3.1.3 is used. For both approaches, a damping ratio of 2% is assigned to the first two modes of both frames, and the time step is set to the one recorded in the ground motions (i.e., 0.005 s). Since these two RC frames are not repaired after each ground motion [39], the four ground motions for frame SS1 and the six ground motions for frame SS2 are grouped to be a sequential ground motion that serves as the input ground motion. Note that frame SS1 collapsed under EQ4, and thus, only the first 2.75 s of the experimental results are recorded [39]. The time-history results regarding the time versus roof displacement and the floor versus peak story drift ratio are presented in Figs. 7–10.

Fig. 7 presents the comparison of the predicted time-roof displacement results for frame SS1 between the fiber model and the proposed method, with the experimental data serving as the ground truth. By observation, the proposed method achieves better agreement with the experimental data for all four EQs over the full-time histories. Further, the proposed approach nearly captures the peak roof displacement for all four EQs, while the fiber model underestimates those peak roof displacements. Peak story drift ratio is an important engineering demand parameter (EDP) that is typically used to quantify the seismic performance of an RC structure [3,5,32]. Fig. 8 shows the results of floor versus peak story drift ratio for frame SS1. It can be seen that the proposed approach performs better than the fiber model, where the peak

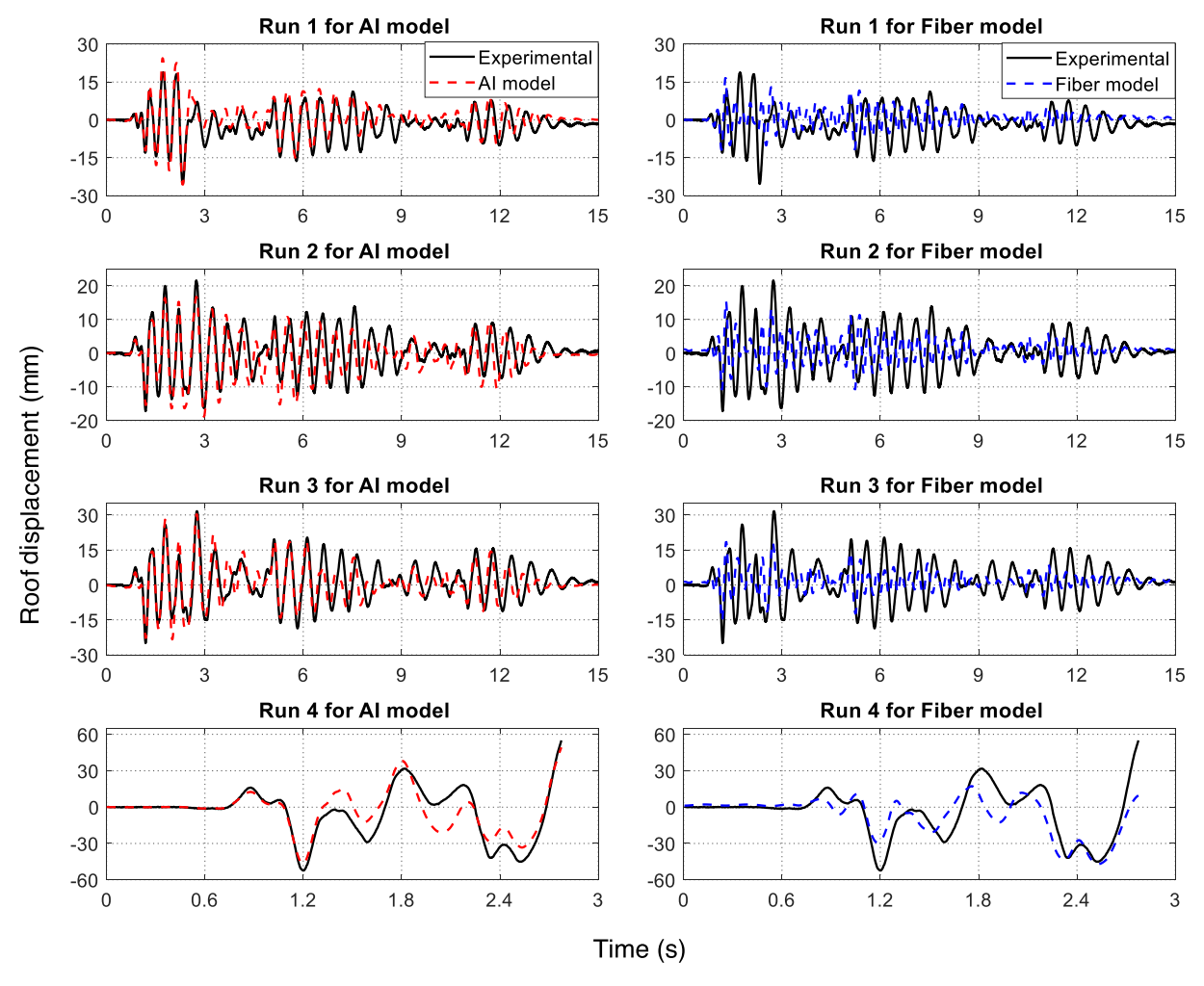


Fig. 7. Time vs. roof displacement results of frame SS1 for the traditional fiber-based modeling approach (i.e., fiber model) and the proposed AI-enhanced shear building model (i.e., AI model), with the experimental data serving as the ground truth.

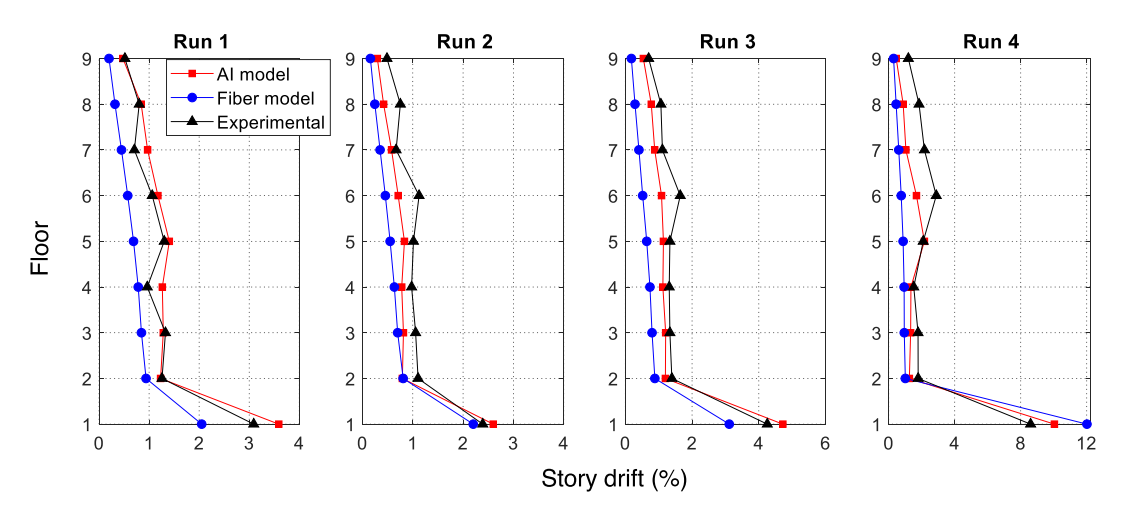


Fig. 8. Distribution of peak story drift ratio along the floors for the traditional fiber-based modeling approach (i.e., fiber model) and the proposed AI-enhanced shear building model (i.e., AI model), with the experimental data serving as the ground truth.

story drift ratios predicted by the proposed approach at each floor for all four EQs have a closer agreement with the experimental results than those predicted by the fiber model. A similar trend is observed by the comparison of the results of the predicted time-roof displacement for frame SS2, as shown in Fig. 9. The proposed approach also accurately

captures the peak roof displacements for all six EQs, while the fiber model over-underestimates these values. Additionally, for the comparison of the predicted peak drift ratios at the second through ninth floors, the proposed method shows better agreement with the experimental data for all six ground motions than the fiber model (Fig. 10). However,

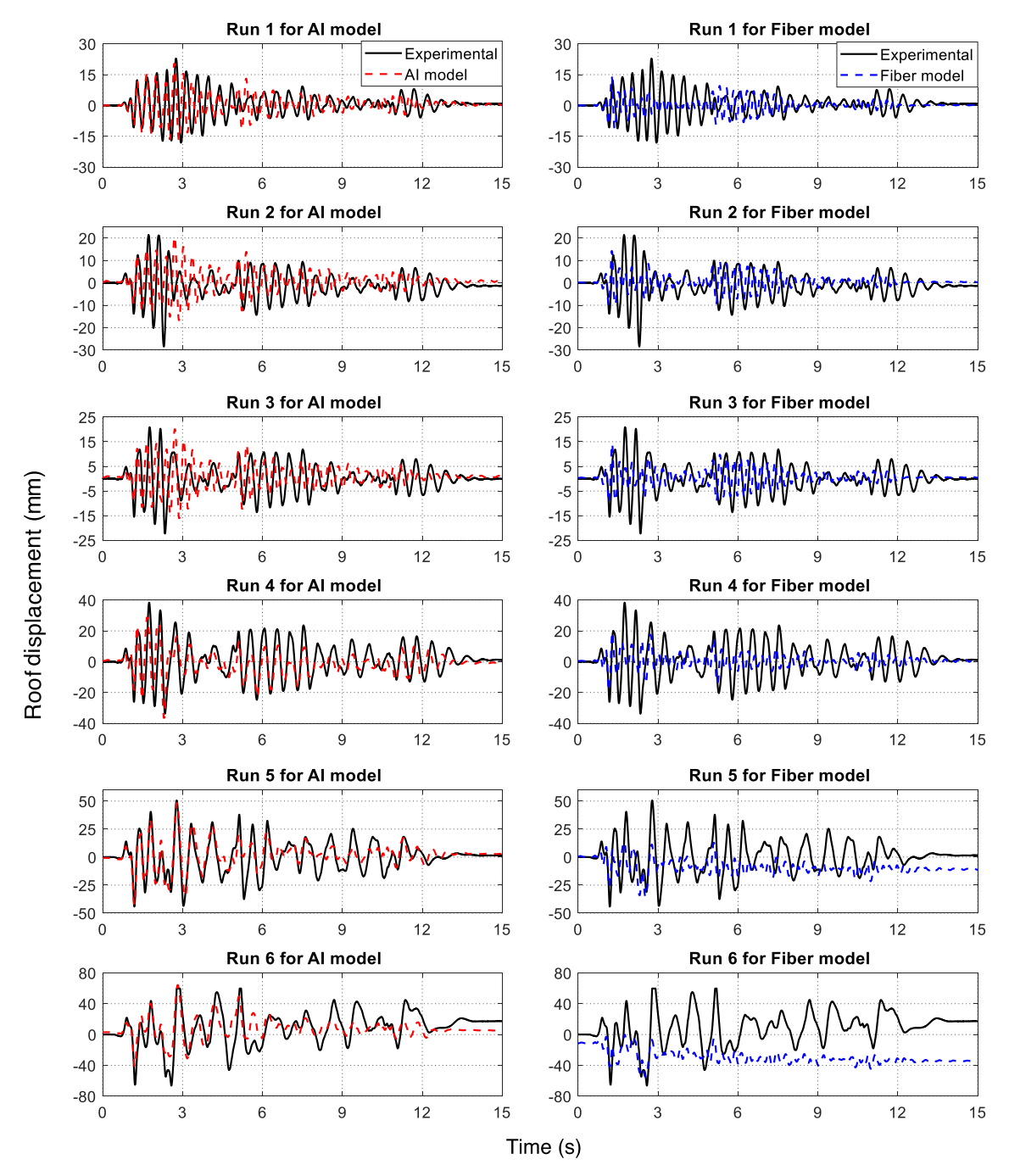


Fig. 9. Time vs. roof displacement results of frame SS2 for the traditional fiber-based modeling approach (i.e., fiber model) and the proposed AI-enhanced shear building model (i.e., AI model), with the experimental data serving as the ground truth.

for the predicted peak drift ratios at the first floor, compared to the proposed method, the fiber model achieves a closer agreement with the experimental results for EQ3 through EQ5 and has comparable performance for EQ1, EQ2, and EQ6. Further, both the fiber model and the proposed approach show discrepancy with the experimental results for the predicted peak drift ratios at the first and seventh through ninth floors for EQ5 and EQ6, where the PGA for EQ5 is 1.06 g and for EQ6 is 1.30 g. Besides, both methods underestimate the story drift for all stories except for the first story. This could be due to the fact that the numerical models established by both methods have higher stiffness for all stories except for the first story, leading to smaller displacement amplitudes and story drifts for these stories in comparison to the experimental data.

Statistical indicators including root mean square error (RMSE) and mean absolute error (MAE) are used to comprehensively quantify the performance of the proposed approach. A method performs very well when the RMSE and MAE values are very small and close to 0. Table 3 presents the detailed performance comparison between the proposed method and fiber-based modeling approach in terms of RMSE and MAE metrics, where they are computed based on all nine floors' peak drift ratio results. As seen in Table 3, the proposed approach achieves the best performance for all four runs in the case of frame SS1, since the RMSE and MAE values for the proposed approach are much lower than those for the fiber-based method. Notably, for Run 1 in frame SS1, in comparison to the fiber-based method, the proposed approach significantly improves the predictive performance by reducing RMSE and MAE values by almost 58% and 66%, respectively. For frame SS2 subjected to the first three earthquakes (i.e., Runs 1–3), the proposed approach performs much better than the fiber-based modeling method by significantly

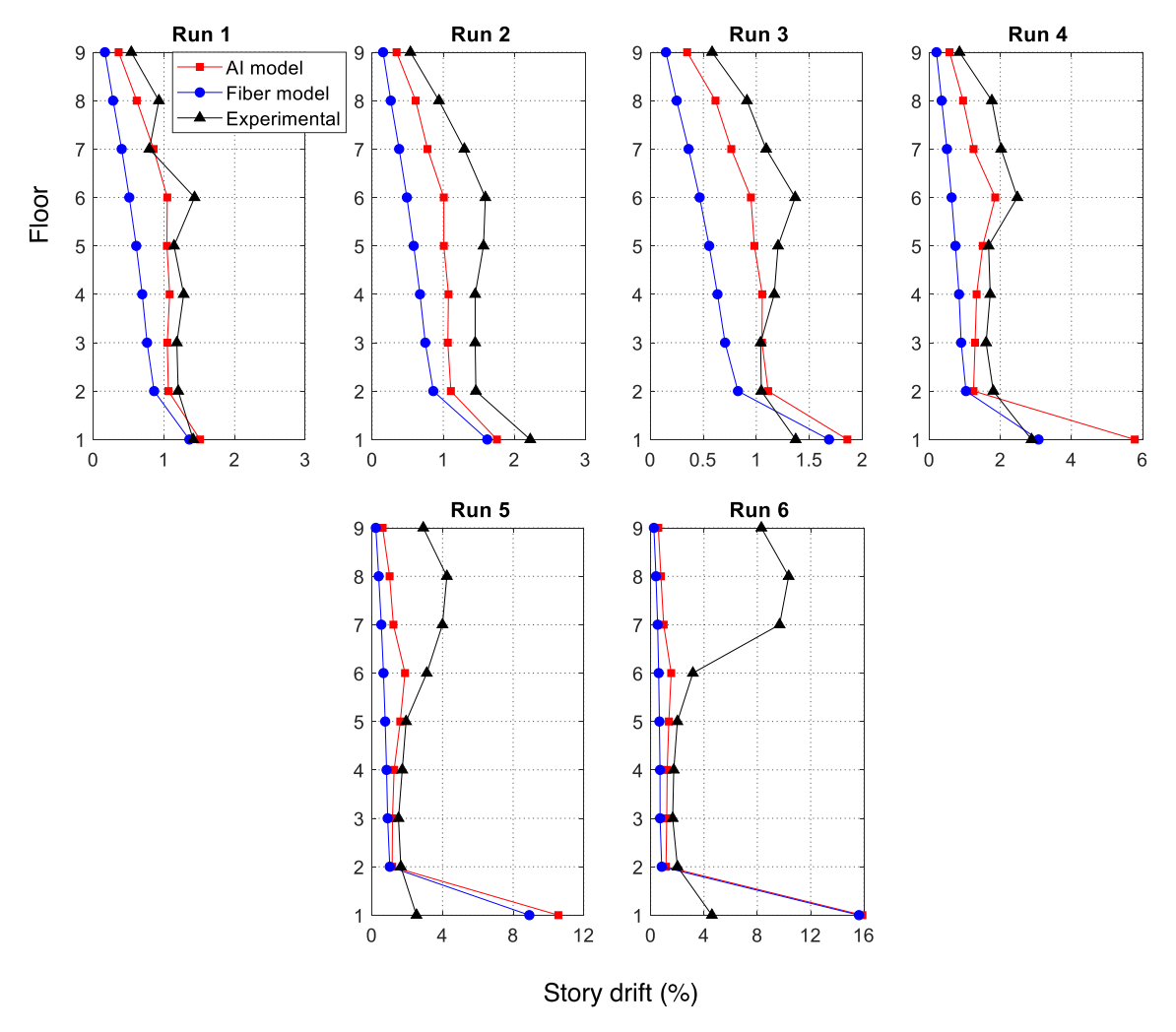


Fig. 10. Distribution of peak story drift ratio along the floors for the traditional fiber-based modeling approach (i.e., fiber model) and the proposed AI-enhanced shear building model (i.e., AI model), with the experimental data serving as the ground truth.

Table 3

Performance comparison between the proposed method and fiber-based modeling approach for peak story drift prediction of RC frames SS1 subjected to four earthquakes and SS2 under six earthquakes. Bold values represent the best performance.

Model	Performance	Frame SS	Frame SS1			Frame SS2					
		Run1	Run2	Run3	Run4	Run1	Run2	Run3	Run4	Run5	Run6
Proposed Method	RMSE (%)	0.22	0.26	0.30	0.87	0.21	0.43	0.28	1.09	3.16	6.32
	MAE (%)	0.16	0.24	0.27	0.74	0.18	0.42	0.24	0.76	2.13	4.60
Fiber-based Method	RMSE (%)	0.52	0.41	0.77	1.65	0.53	0.78	0.57	1.10	3.05	6.51
	MAE (%)	0.46	0.39	0.73	1.42	0.47	0.75	0.53	0.99	2.46	5.03

enhancing the predictive accuracy, where the proposed approach roughly results in 60% and 62% reductions for RMSE and MAE values, respectively in comparison with fiber-based modeling method in the case of Run 1. However, for frame SS2 subjected to the last three earthquakes (i.e., Runs 4–6), the performance improvement is not significant. This is because under extreme seismic intensities, the behavior of frame SS2 becomes more irregular, and higher modes other than the first are seen to have a greater effect on displacement response, as discussed in Schultz [39]. Both the fiber model and the proposed method consider the first two modes more heavily than others, finally leading to significant errors. Additionally, the sample size of the training set may not be sufficient to train an AI model that can precisely capture the high nonlinearity of frame SS2 under large earthquakes. Nevertheless, in most cases, the proposed approach still achieves better agreement with the experimental data than the traditional fiber model, as validated in

# Table 3.

Additionally, the computational time for all ground motions using the proposed approach only requires 133 (frame SS1) and 289 (frame SS2) seconds. This time is substantially diminished when compared to the fiber models which took 972 (frame SS1) and 1,942 (frame SS2) seconds. Thus, the proposed approach significantly enhances computational efficiency while still maintaining good prediction performance. Further, the fiber model is implemented using OpenSees, which is developed using compiled language (i.e., C++), while the proposed approach is implemented using Matlab, which is an interpreted language. Thus, OpenSees is inherently faster than Matlab. However, the proposed approach is still much more efficient than the fiber model. In the future, a compiled language (e.g., C++) will be used to implement the proposed approach, and it is expected to have a faster computational procedure. Based on these comparisons, the proposed approach

presented in this paper performs significantly better than the traditional fiber-based modeling method for all seismic response quantities and agrees better with the experimental data.

# 5.3. Discussion of results

The results obtained for both displacement-controlled quasi-static cyclic loading and shake table tests suggest that the proposed AIenhanced shear building model outperforms the classical fiber-based modeling approach in predicting the seismic response history of RC frames in terms of both prediction capability and computational efficiency. For the displacement-controlled quasi-static cyclic loading test, the results validate that the proposed approach can reasonably and efficiently predict the hysteretic behaviors of all stories of the RC frame subjected to cyclic loading reversals, including pinching behavior, stiffness and strength deterioration. This is because physical experimental data of RC columns is used in developing the hysteretic modeler for each column in the target RC frame. Therefore, it is expected that the hysteretic modeler can accurately and reasonably estimate the lateral stiffness of each column in the target RC frame, which is then utilized to formulate the structural stiffness matrix for seismic response calculation of the target RC frame under cyclic loading reversals.

For the shake table tests, the results demonstrate that the proposed approach can reasonably and efficiently predict the seismic response history and estimate the peak story drift of RC frames under moderate and large earthquakes. The results predicted by the proposed approach for frame SS1 have a closer agreement with the experimental data than those for frame SS2. This is because the columns in frame SS2 have a higher longitudinal reinforcement ratio than those in frame SS1, which means that the columns in frame SS2 are stiffer than those in frame SS1. In this way, frame SS1 is more suitable for the proposed method than frame SS2 as the ratio of column stiffness to beam stiffness for frame SS2 is higher than that for frame SS1. Additionally, the comparison of the above results also verified that the proposed approach achieves a good compromise between predictive performance and computational efficiency. This characteristic demonstrates that the proposed approach is a promising computational tool for accurate and efficient seismic response prediction and for other near-real-time scenarios.

# 5.4. Discussion of limitations

Although the proposed AI-enhanced computational method has shown good performance for nonlinear seismic response prediction of RC frames, it does have some limitations. First, the proposed model cannot accurately predict the nonlinear seismic response of frame buildings that have smoother hysteresis curves (e.g., steel frames). This is because the hysteretic model utilized in the proposed method is polygonal where every branch of the hysteretic curve follows a linear relationship. Second, the proposed approach is not appropriate for frame buildings that have a high ratio of column stiffness to beam stiffness. This is because when the ratio of column stiffness to beam stiffness is high, the beam cannot be regarded as rigid in flexure, leading to floor rotation. This is incompatible with the assumption made in the proposed method that only translational displacement is considered at the floor level. Finally, because the proposed AI-enhanced model contains an AI technique, some properties that AI methods have are also applicable to the proposed method. Like all AI methods, the proposed approach can accurately predict the hysteretic parameters of RC columns within the input ranges of the training set (the 272 rectangular RC column specimens). Outside of these ranges, it cannot necessarily reliably be used for hysteretic parameter prediction of RC columns.

#### 6. Conclusions

A novel AI-enhanced computational method is proposed to predict nonlinear seismic response of RC frames under displacement-controlled quasi-static cyclic loading and dynamic earthquake ground motions. The proposed approach incorporates an AI technique with the shear building model, which leverages the advantages of both the AI technique and the shear building model to achieve accurate and efficient predictions. To validate the performance of the proposed approach and demonstrate the novel contributions of the method, two illustrative examples, one for quasi-static cyclic loading and another for dynamic earthquake ground motions, are presented based on a database of 272 rectangular RC column specimens. The numerical results of the first example validate that the proposed approach can accurately and efficiently predict the nonlinear seismic behavior including yield force, peak force, drift capacity, and hysteretic energy dissipation for each story of RC frame under quasi-static cyclic loading. For the second example, the numerical results demonstrate that the proposed approach is able to accurately and efficiently predict the nonlinear seismic response of RC frames under moderate and large earthquakes and reasonably capture their peak story drift. Further, for both examples, the proposed approach outperforms the classical fiber-based modeling method in both predictive capability and computational efficiency, yielding the great potential for near-realtime needs.

# **Declaration of Competing Interest**

The authors declare that they have no known competing financial interests or personal relationships that could have appeared to influence the work reported in this paper.

#### Acknowledgements

This material is based in part upon work supported by the National Science Foundation under the grant CMMI #1944301. Any opinions, findings, and conclusions or recommendations expressed in this material are those of the authors and do not necessarily reflect the views of the National Science Foundation.

#### References

- H. Adeli, Neural networks in civil engineering: 1989–2000, Comput.-Aided Civ. Infrastruct. Eng. 16 (2) (2001) 126–142.
- [2] M. Berry, M. Parrish, M. Eberhard, PEER Structural Performance Database, User's Manual (Version 1.0), University of California, Berkeley, 2004.
- [3] J.M. Bracci, S.K. Kunnath, A.M. Reinhorn, Seismic performance and retrofit evaluation of reinforced concrete structures, J. Struct. Eng. 123 (1) (1997) 3–10.
- [4] H. Cecen, Response of Ten-Story Reinforced Concrete Frames to Simulated Earthquakes (Doctoral dissertation), Doctoral Dissertation, Graduate College, University of Illinois, Urbana, 1979.
- [5] A.K. Chopra, Dynamics of structures: theory and applications to earthquake engineering, Prentice Hall, 2007.
- [6] J.-S. Chou, N.-T. Ngo, A.-D. Pham, Shear strength prediction in reinforced concrete deep beams using nature-inspired metaheuristic support vector regression, J. Comput. Civil Eng. 30 (1) (2016) 04015002, https://doi.org/10.1061/(ASCE) CP.1943-5487.0000466.
- [7] G.G. Deierlein, A.M. Reinhorn, M.R. Willford, Nonlinear structural analysis for seismic design, NEHRP Seismic Design Technical Brief 4 (2010) 1–36.
- [8] K.J. Elwood, J.P. Moehle, Drift capacity of reinforced concrete columns with light transverse reinforcement, Earthquake Spectra 21 (1) (2005) 71–89.
- [9] T.-S. Eom, S.-M. Kang, H.-G. Park, T.-W. Choi, J.-M. Jin, Cyclic loading test for reinforced concrete columns with continuous rectangular and polygonal hoops, Eng. Struct. 67 (2014) 39–49.
- [10] D.-C. Feng, Z.-T. Liu, X.-D. Wang, Z.-M. Jiang, S.-X. Liang, Failure mode classification and bearing capacity prediction for reinforced concrete columns based on ensemble machine learning algorithm, Adv. Eng. Inf. 45 (2020) 101126, https://doi.org/10.1016/j.aei.2020.101126.
- [11] D.-C. Feng, W.-J. Wang, S. Mangalathu, G. Hu, T. Wu, Implementing ensemble learning methods to predict the shear strength of RC deep beams with/without web reinforcements, Eng. Struct. 235 (2021) 111979, https://doi.org/10.1016/j. engstruct.2021.111979.
- [12] S. German, I. Brilakis, R. DesRoches, Rapid entropy-based detection and properties measurement of concrete spalling with machine vision for post-earthquake safety assessments, Adv. Eng. Inf. 26 (4) (2012) 846–858.
- [13] S. German, J.-S. Jeon, Z. Zhu, C. Bearman, I. Brilakis, R. DesRoches, L. Lowes, Machine vision-enhanced postearthquake inspection, J. Comput. Civil Eng. 27 (6) (2013) 622–634.
- [14] J.A. Goulet, C. Michel, A.D. Kiureghian, Data-driven post-earthquake rapid structural safety assessment, Earthquake Eng. Struct. Dyn. 44 (4) (2015) 549–562.

- [15] P. Grossi, H. Kunreuther (Eds.), Catastrophe ModelingCatastrophe Modeling: A New Approach to Managing Risk, Kluwer Academic Publishers, Boston, 2005.
- [16] R. Guarize, N.A.F. Matos, L.V.S. Sagrilo, E.C.P. Lima, Neural networks in the dynamic response analysis of slender marine structures, Appl. Ocean Res. 29 (4) (2007) 191–198.
- [17] N.-D. Hoang, X.-L. Tran, H. Nguyen, Predicting ultimate bond strength of corroded reinforcement and surrounding concrete using a metaheuristic optimized least squares support vector regression model, Neural Comput. Appl. 32 (11) (2020) 7289–7309.
- [18] C. Koch, S.G. Paal, A. Rashidi, Z. Zhu, M. König, I. Brilakis, Achievements and challenges in machine vision-based inspection of large concrete structures, Adv. Struct. Eng. 17 (3) (2014) 303–318.
- [19] N.D. Lagaros, M. Papadrakakis, Neural network based prediction schemes of the non-linear seismic response of 3D buildings, Adv. Eng. Softw. 44 (1) (2012) 92–115.
- [20] D. Lattanzi, G.R. Miller, M.O. Eberhard, O.S. Haraldsson, Bridge column maximum drift estimation via computer vision, J. Comput. Civil Eng. 30 (4) (2016) 04015051, https://doi.org/10.1061/(ASCE)CP.1943-5487.0000527.
- [21] H. Luo, S.G. Paal, Machine learning-based backbone curve model of reinforced concrete columns subjected to cyclic loading reversals, J. Comput. Civil Eng. 32 (5) (2018) 04018042, https://doi.org/10.1061/(ASCE)CP.1943-5487.0000787.
- [22] H. Luo, S.G. Paal, A locally weighted machine learning model for generalized prediction of drift capacity in seismic vulnerability assessments, Comput.-Aided Civ. Infrastruct. Eng. 34 (11) (2019) 935–950.
- [23] H. Luo, S.G. Paal, Reducing the effect of sample bias for small data sets with double-weighted support vector transfer regression, Comput.-Aided Civ. Infrastruct. Eng. 36 (3) (2021) 248–263.
- [24] H. Luo, S.G. Paal, Advancing post-earthquake structural evaluations via sequential regression-based predictive mean matching for enhanced forecasting in the context of missing data, Adv. Eng. Inf. 47 (2021) 101202, https://doi.org/10.1016/j. aei 2020 101202
- [25] H. Luo, S.G. Paal, Data-driven seismic response prediction of structural components. 87552930211053345, Earthquake Spectra (2021).
- [26] J.B. Mander, M.J.N. Priestley, R. Park, Theoretical stress-strain model for confined concrete, J. Struct. Eng. 114 (8) (1988) 1804–1826.
- [27] S. Mangalathu, J.-S. Jeon, Machine Learning-Based Failure Mode Recognition of Circular Reinforced Concrete Bridge Columns: Comparative Study, J. Struct. Eng. 145 (10) (2019) 04019104, https://doi.org/10.1061/(ASCE)ST.1943-541X.0002402.
- [28] S. Mangalathu, J.-S. Jeon, R. DesRoches, Critical uncertainty parameters influencing seismic performance of bridges using Lasso regression, Earthquake Eng. Struct. Dyn. 47 (3) (2018) 784–801.
- [29] A. Marini, E. Spacone, Analysis of reinforced concrete elements including shear effects, ACI Struct. J. 103 (5) (2006) 645.
- [30] F. McKenna, G.L. Fenves, M.H. Scott, Open system for earthquake engineering simulation, University of California, Berkeley, CA, 2000.
- [31] M. Menegotto, P. Pinto, Method of analysis for cyclically loaded R.C. plane frames including changes in geometry and non-elastic behavior of elements under combined normal force and bending, International Association for Bridge and Structural Engineering, Lisbon, Portugal, 1973.
- [32] J. Moehle, G.G. Deierlein, A framework methodology for performance-based earthquake engineering, 13th world conference on earthquake engineering vol. 679 (2004).
- [33] J. Moehle, Seismic design of reinforced concrete buildings, McGraw Hill Professional, 2014.
- [34] F.J. Montáns, F. Chinesta, R. Gómez-Bombarelli, J.N. Kutz, Data-driven modeling and learning in science and engineering, Comptes Rendus Mécanique 347 (11) (2019) 845–855
- [35] S.G. Paal, J.-S. Jeon, I. Brilakis, R. DesRoches, Automated damage index estimation of reinforced concrete columns for post-earthquake evaluations, J. Struct. Eng. 141 (9) (2015) 04014228, https://doi.org/10.1061/(ASCE)ST.1943-541X.0001200.

- [36] M. Pal, S. Deswal, Support vector regression based shear strength modelling of deep beams, Comput. Struct. 89 (13-14) (2011) 1430–1439.
- [37] Y. Reich, Machine learning techniques for civil engineering problems, Comput-Aided Civ. Infrastruct. Eng. 12 (4) (1997) 295–310.
- [38] B. Scott, R. Park, M. Priestley, Stress-strain behavior of concrete confined by overlapping hoops at low and high strain rates, ACI J. Proc. 79 (1) (1982) 13–27.
- [39] A.E. Schultz, An experimental and analytical study of the earthquake response of R/C frames with yielding columns (Doctoral dissertation), University of Illinois at Urbana-Champaign, 1986.
- [40] H. Sezen, J.P. Moehle, Shear strength model for lightly reinforced concrete columns, J. Struct. Eng. 130 (11) (2004) 1692–1703.
- [41] E. Spacone, F.C. Filippou, F.F. Taucer, Fibre beam-column model for non-linear analysis of R/C frames: Part I. Formulation, Earthquake Eng. Struct. Dyn. 25 (7) (1996) 711–725.
- [42] E. Spacone, F.C. Filippou, F.F. Taucer, Fibre beam-column model for non-linear analysis of r/c frames: part ii. applications, Earthquake Eng. Struct. Dyn. 25 (7) (1996) 727-742.
- [43] J. Suykens, T. Van Gestel, J. De Brabanter, B. De Moor, J. Vandewalle, Least Squares Support Vector Machines, World Scientific, 2002.
- [44] F. Taucer, E. Spacone, F.C. Filippou, A fiber beam-column element for seismic response analysis of reinforced concrete structures, vol. 91, no. 17, Earthquake Engineering Research Center, College of Engineering, University of California, Berkekey, California, 1991.
- [45] V.N. Vapnik (Ed.), The Nature of Statistical Learning Theory, Springer New York, New York, NY, 1995.
- [46] G.M. Verderame, G. Fabbrocino, G. Manfredi, Seismic response of rc columns with smooth reinforcement. Part II: Cyclic tests, Eng. Struct. 30 (9) (2008) 2289–2300.
- [47] D.-T. Vu, N.-D. Hoang, Punching shear capacity estimation of FRP-reinforced concrete slabs using a hybrid machine learning approach, Struct. Infrastruct. Eng. 12 (9) (2016) 1153–1161.
- [48] R.-T. Wu, M.R. Jahanshahi, Deep convolutional neural network for structural dynamic response estimation and system identification, J. Eng. Mech. 145 (1) (2019) 04018125, https://doi.org/10.1061/(ASCE)EM.1943-7889.0001556.
- [49] Y. Xie, M. Ebad Sichani, J.E. Padgett, R. DesRoches, The promise of implementing machine learning in earthquake engineering: A state-of-the-art review, Earthquake Spectra 36 (2020) 1769–1801.
- [50] L. Xie, X. Lu, H. Guan, X. Lu, Experimental study and numerical model calibration for earthquake-induced collapse of RC frames with emphasis on key columns, joints, and the overall structure, J. Earthquake Eng. 19 (8) (2015) 1320–1344.
- [51] Y. Yu, H. Yao, Y. Liu, Structural dynamics simulation using a novel physics-guided machine learning method, Eng. Appl. Artif. Intell. 96 (2020) 103947, https://doi. org/10.1016/j.engappai.2020.103947.
- [52] Y.u. Zhang, H.V. Burton, H. Sun, M. Shokrabadi, A machine learning framework for assessing post-earthquake structural safety, Struct. Saf. 72 (2018) 1–16.
- [53] R. Zhang, Z. Chen, S.u. Chen, J. Zheng, O. Büyüköztürk, H. Sun, Deep long short-term memory networks for nonlinear structural seismic response prediction, Comput. Struct. 220 (2019) 55–68.
- [54] R. Zhang, Y. Liu, H. Sun, Physics-guided convolutional neural network (PhyCNN) for data-driven seismic response modeling, Eng. Struct. 215 (2020) 110704, https://doi.org/10.1016/j.engstruct.2020.110704.
- [55] Z. Zhu, S. German, I. Brilakis, Visual retrieval of concrete crack properties for automated post-earthquake structural safety evaluation, Autom. Constr. 20 (7) (2011) 874–883.
- [56] H. Luo, S.G. Paal, A data-free, support vector machine-based physics-driven estimator for dynamic response computation, Comput.-Aided Civ. Infrastruct. Eng. (2022) 1–23, https://doi.org/10.1111/mice.12823.
- [57] Yan Zhou, Experimental investigation into the seismic behavior of squat reinforced concrete walls subjected to acid rain erosion. Journal of Building Engineering 44 (2021) 102899.
- [58] Jiulin Bai, Huiming Chen, Junxian Zhao, Seismic design and subassemblage tests of buckling-restrained braced RC frames with shear connector gusset connections, Engineering Structures 234 (2021) 112018.